Original Article
Yonsei Med J 2021 May;62(5):431-438
https://doi.org/10.3349/ymj.2021.62.5.431
Yonsei Medical Journal
YMJ
pISSN: 0513-5796 · eISSN: 1976-2437

Clinical Features and Brain MRI Findings in Korean Patients with AGel Amyloidosis

E-Nae Cheong[1,2*], Wooyul Paik[3*], Young-Chul Choi[4], Young-Min Lim[5], Hyunjin Kim[5], Woo Hyun Shim[1,2,6], and Hyung Jun Park[4,7]

[1]Asan Institute for Life Sciences, Asan Medical Center, University of Ulsan College of Medicine, Seoul;
[2]Department of Medical Science and Asan Medical Institute of Convergence Science and Technology, Asan Medical Center, University of Ulsan College of Medicine, Seoul;
Departments of [3]Radiology and [7]Neurology, Gangneung Asan Hospital, University of Ulsan College of Medicine, Gangneung;
[4]Department of Neurology, Rehabilitation Institute of Neuromuscular Disease, Gangnam Severance Hospital, Yonsei University College of Medicine, Seoul;
Departments of [5]Neurology and [6]Radiology, Asan Medical Center, University of Ulsan College of Medicine, Seoul, Korea.

Purpose: AGel amyloidosis is systemic amyloidosis caused by pathogenic variants in the *GSN* gene. In this study, we sought to characterize the clinical and brain magnetic resonance image (MRI) features of Korean patients with AGel amyloidosis.
Materials and Methods: We examined 13 patients with AGel amyloidosis from three unrelated families. Brain MRIs were performed in eight patients and eight age- and sex-matched healthy controls. Therein, we analyzed gray and white matter content using voxel-based morphometry (VBM), tract-based spatial statistics (TBSS), and FreeSurfer.
Results: The median age at examination was 73 (interquartile range: 64–76) years. The median age at onset of cutis laxa was 20 (interquartile range: 15–30) years. All patients over that age of 60 years had dysarthria, cutis laxa, dysphagia, and facial palsy. Two patients in their 30s had only mild cutis laxa. The median age at dysarthria onset was 66 (interquartile range: 63.5–70) years. Ophthalmoparesis was observed in three patients. No patient presented with muscle weakness of the limbs. Axial fluid-attenuated inversion recovery images of the brain showed no significant differences between the patient and control groups. Also, analysis of VBM, TBSS, and FreeSurfer revealed no significant differences in cortical thickness between patients and healthy controls at the corrected significance level.
Conclusion: Our study outlines the clinical manifestations of prominent bulbar palsy and early-onset cutis laxa in 13 Korean patients with AGel amyloidosis and confirms that AGel amyloidosis mainly affects the peripheral nervous system rather than the central nervous system.

Key Words: AGel amyloidosis, gelsolin-related amyloidosis, gelsolin, GSN, brain, diffusion tensor imaging

INTRODUCTION

AGel amyloidosis is an autosomal dominant form of systemic amyloidosis caused by pathogenic variants in the *GSN* gene.[1] AGel amyloidosis was first observed by the Finnish ophthalmologist Jouko Meretoja, and it is one of the most common ge-

Received: September 21, 2020 **Revised:** February 2, 2021 **Accepted:** February 9, 2021
Co-corresponding authors: Hyung Jun Park, MD, PhD, Department of Neurology, Gangnam Severance Hospital, Yonsei University College of Medicine, 211 Eonju-ro, Gangnam-gu, Seoul 06273, Korea.
Tel: 82-2-2019-3329, Fax: 82-2-3462-5904, E-mail: hjpark316@yuhs.ac and
Woo Hyun Shim, PhD, Department of Medical Science and Asan Medical Institute of Convergence Science and Technology, Asan Medical Center, University of Ulsan College of Medicine, 88 Olympic-ro 43-gil, Songpa-gu, Seoul 05505, Korea.
Tel: 82-2-3010-2775, Fax: 82-2-3010-8634, E-mail: swh@amc.seoul.kr

*E-Nae Cheong and Wooyul Paik contributed equally to this work.
•The authors have no potential conflicts of interest to disclose.

netic disorders of the Finnish disease heritage.[2,3] There are two common pathogenic variants in the *GSN* gene (NM_000177.5: c.640G>A and c.640G>T). The c.640G>A variant (NP_000168.1: p.D214N) is the most common and has been observed in Finland, Germany, Great Britain, Iran, Japan, Netherlands, Portugal, Spain, Sweden, and the United States.[4-13] The c.640G>T variant (NP_000168.1: p.D214Y) is less common and has been reported in Denmark, Brazil, Czechoslovakia, France, Korea, and the United States.[5,14-18]

Typical clinical features of AGel amyloidosis include cranial and peripheral neuropathy, cutis laxa, and corneal lattice amyloidosis. The most common neurological symptoms are facial neuropathy and polyneuropathy, followed by myokymia, hearing impairment, carpal tunnel syndrome, ataxia, and dysarthria.[3] However, a previous study reported severe bulbar dysfunction in one family with the c.640G>T variant.[18] AGel amyloidosis is a systemic disease frequently involving the peripheral nervous system, and there have been few studies on its involvement in the central nervous system.[19,20] Therefore, we suspect that additional cerebral abnormalities, particularly in the corticobulbar tract, may appear in patients with AGel amyloidosis.

Recent advancements in the evaluation of the magnitude and directionality of water diffusion using diffusion tensor imaging (DTI) have made it possible to visualize nerve fiber orientation and the microstructural integrity of brain tissues. The use of quantitative measurements obtained using DTI can indicate the disruption of white matter (WM) integrity, which cannot be identified using conventional magnetic resonance imaging (MRI) techniques.[21,22] In addition, voxel-based morphometry (VBM) can be used to assess whole-brain morphology using anatomical MRI without prior hypothesis about possible changes in a brain region. The VBM method can highlight the intact and damaged areas of the brain by assigning a constant signal intensity value to each voxel and the associated neural differences in a target group. Therefore, DTI and VBM have been widely applied to investigate cerebral abnormalities in patients with various diseases, including Alzheimer's disease, Parkinson's disease, and neuromuscular disorders.[23-27]

Our study aimed to analyze the clinical and genetic features of Korean patients and to examine the presence of cerebral abnormalities in patients with AGel amyloidosis. Herein, we summarized the clinical characteristics of 13 Korean patients with AGel amyloidosis. We also analyzed the extent of WM and gray matter (GM) alterations in these patients using multimodal voxel-wise methods.

MATERIALS AND METHODS

Study participants

We reviewed the medical records of Gangneung Asan Hospital from March 2018 to September 2019. In doing so, 13 patients from three unrelated families were found to have AGel amyloidosis (III-6, III-7, III-9, III-10, and III-14 from MF1531; II-6, III-2, III-3, IV-1, and IV-2 from MF1532; and III-2, III-3, and III-5 from MF1533) (Fig. 1A). All patients had a pathogenic variant in *GSN* (NM_000177.5: c.640G>T; NP_000168.1: p.D214Y), which was completely co-segregated in the affected individuals from three families (Fig. 1B): this variant was previously identified as a pathogenic variant.[28] We analyzed the clinical spectrum of the patients, including sex, age at diagnosis, age at symptom onset, and the presence of cutis laxa, drooping eyelids, cranial nerve functions, motor weakness, and sensory deficits. We examined eye movements in the nine cardinal positions of gaze. Motor weakness was evaluated by manual muscle testing. We also evaluated pain sense with a pin test, vibration sense with a 128-Hz tuning fork, and joint position sense at the interphalangeal joint of the big toe. Laboratory and radiological tests included slip lamp, nerve conduction, needle electromyography, and brain MRI studies. The Institutional Review Board of Gangneung Asan Hospital approved the current study (approval number: 2019-06-040). All personal information was anonymously encrypted.

Brain MRI acquisition and analysis protocol

Eight patients with AGel amyloidosis and eight age- and sex-matched healthy controls underwent brain MRI. The healthy controls did not present with any neuromuscular disorders and were referred to our hospital due to headaches. MRI data were obtained with a 3T scanner (Magnetom Skyra; Siemens, Munich, Germany) using a 20-channel head-neck coil. Based on the anatomical images of localization, T1-MPRAGE (TR: 1810 ms, TE: 2.81 ms, and thickness: 1 mm) sagittal images and fluid-attenuated inversion recovery (FLAIR) (TR: 9,000 ms, TE: 76 ms, and thickness: 5 mm) axial images covering the whole brain were acquired. Meanwhile, DTI data were obtained with a single-shot echo-planar imaging sequence (TR: 8,000 ms, TE: 74 ms, matrix: 100×100, voxel size: 2.2×2.2×2.5 mm^3, gradient orientations: 64, and b-value: 1,000 s/mm^2). The measured raw DICOM data were converted into the NIFTI format using dcm2nii, which is part of the neuroimaging tool MRIcron.

VBM analysis

VBM was performed using SPM 12 (Wellcome Department of Cognitive Neurology, https://fsl.fmrib.ox.ac.uk/fsl/fslwiki/FSLVBM) and the Diffeomorphic Anatomical Registration using Exponentiated Lie Algebra (DARTEL) registration method.[29] Briefly, the T1-weighted images were segmented to produce tissue probability maps in the Montreal Neurological Institute (MNI) space: GM, WM, and cerebrospinal fluid. Then, DARTEL templates were created for registration and normalization from the individually segmented images. GM and WM images were then normalized to the DARTEL templates. Before statistical calculation, the normalized images were smoothed with an 8-mm full-width half-maximum Gaussian filter to increase the signal-to-noise ratio.

https://doi.org/10.3349/ymj.2021.62.5.431

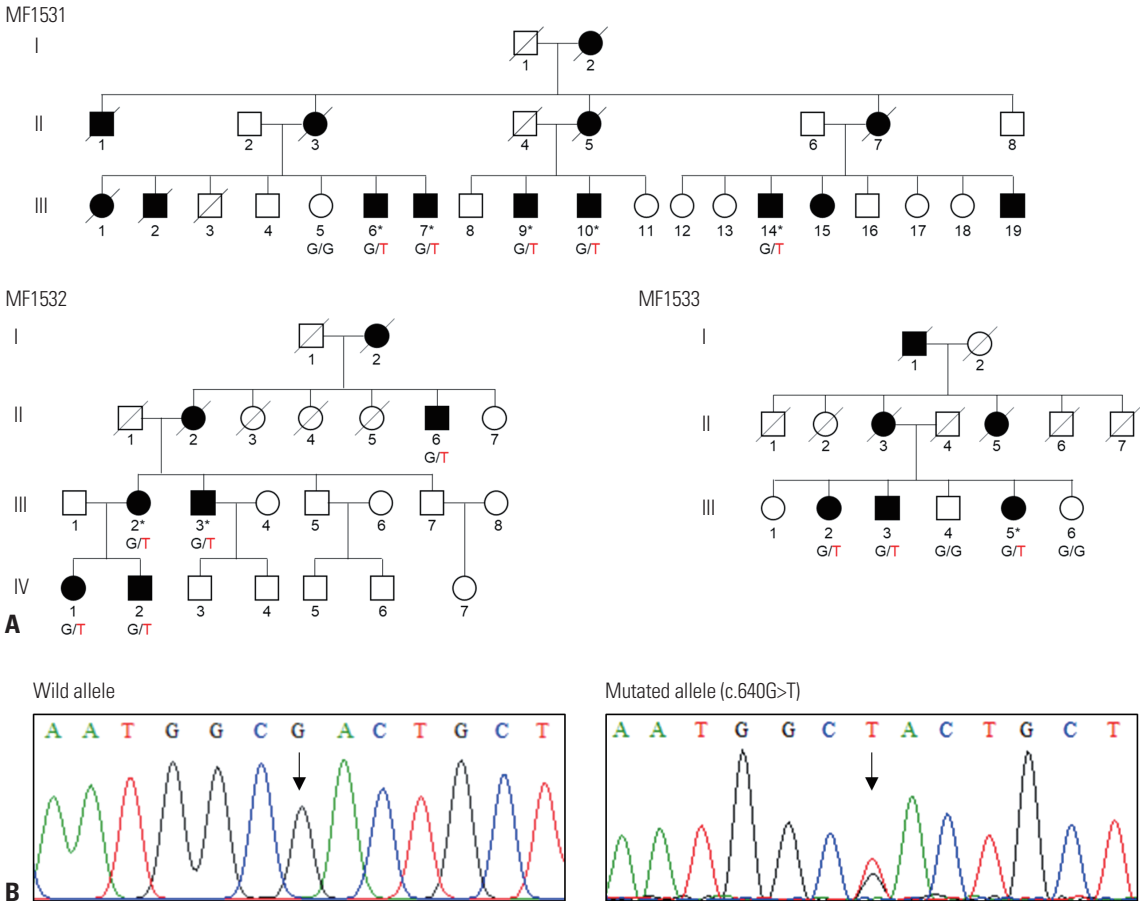

Fig. 1. Pedigree and sequencing chromatograms of three families with AGel amyloidosis. (A) Pedigree of the three families with AGel amyloidosis. Asterisks (*) indicate individuals who participated in the current study. Genotypes of *GSN* (c.640 G>T) are shown under each subject (arrow, proband; square, male; circle, female; filled, affected; not filled, unaffected; diagonal bar across the symbol, deceased). (B) Sequencing chromatograms of the c.640G>A pathogenic variant in *GSN*. This heterozygous variant was completely co-segregated in the affected individuals from three families and was previously identified and classified as a pathogenic variant.

SnPM 13 (Statistical NonParametric Mapping; http://nisox.org/Software/SnPM13/) with 5000 permutations without variance smoothing was used to compare voxel-wise differences in GM volumes between the patients with AGel amyloidosis and healthy controls. Analyses were performed using a linear regression model considering age, sex, and total intracranial volume as covariates. Significant differences were identified using a false discovery rate (FDR)-corrected threshold of $p<0.05$ and an uncorrected threshold of $p<0.001$ ($t>3.69$).

Analysis of tract-based spatial statistics

The processing of diffusion tensor images was performed using software tools from the FMRIB software library (FSL, http://www.fmrib.ox.ac.uk/fsl). Then, a voxel-wise statistical analysis of fractional anisotropy (FA) data was performed using tract-based spatial statistics (TBSS), which is a part of the FSL. Head motion and eddy currents were corrected using the reference B0 image. In addition, brain extraction was conducted using the Brain Extraction Tool (a part of FSL). Then, the diffusion tensors were calculated using three b values and gradient directions, and FA maps were finally produced. These were referred to as the preprocessing stages. Next, FA data were aligned into MNI Space using the FMRIB's Nonlinear Image Registration Tool. Then, the mean FA image (threshold of 0.2) was created and thinned to establish a mean FA skeleton that represents the centers of all tracts common to the group. Each subject's aligned FA data were then projected onto this skeleton, and the resulting data were fed into voxel-wise cross-subject statistics. We used 5000 permutations per test, and threshold-free cluster enhancement was used to enhance cluster-like structures without the need for preset clustering thresholds. FDR-corrected p values<0.05 and uncorrected p values<0.05 were considered statistically significant.

Analysis of cortical thickness

Cortical thickness analysis was performed with the FreeSurfer software (version 6.0; http://surfer.nmr.mgh.harvard.edu) using the "recon-all" processing stream. The implemented processing stream included the removal of non-brain tissue, automated Talairach transformation, normalized intensity, tessellation of GM/WM boundaries, automated topology correction, and surface deformation. Then, the cerebral cortex

was parcellated into the anatomical structures. Cortical thickness was computed by finding the shortest distance between a given point on the estimated pial surface and the GM/WM boundary. The thickness measurement of each vertex of the subjects' surface was mapped on a standard spherical coordinate system. The vertex-wise general linear model was applied for group comparison of the cerebral cortical thickness between patients and healthy controls using the FreeSurfer "qdec" tool after surface-based smoothing of 10 mm FWHM. Age and sex were used as covariates in the models. For all comparisons, an FDR correction for multiple comparisons across space was applied. FDR-corrected p values<0.05 were considered statistically significant.

RESULTS

Clinical presentation of Korean patients with AGel amyloidosis

Three index patients (III-9 from MF1531, III-2 from MF1532, and III-5 from MF1533) were referred to our neurology clinic due to dysarthria and dysphagia. Table 1 shows the demographic and clinical characteristics of 13 patients from three unrelated families. The median age at examination was 73 (interquartile range: 64–76) years. The median age at onset of cutis laxa was 20 (interquartile range: 15–30) years. Cutis laxa was found in all patients. All patients first noticed their loose skin on the scalp when they had their haircut, especially when using hair clippers as teenagers. All patients aged over 60 years complained of drooping eyelids. Patients reported that their eyelids began drooping at the median age of 52 (interquartile range: 51–60) years. Among them, five patients (III-6, III-7, and III-9 from MF1531; III-3 from MF1532; and III-5 from MF1533) had blepharoplasty with or without rhytidectomy at 55, 57, 53, 48, and 62 years old, respectively. All patients aged over 60 years complained of dysarthria, drooling, and dysphagia. The median age at dysarthria onset was 66 (interquartile range: 63.5–70) years. Five patients complained of decreased visual acuity that presented in their 30s. However, analysis using a slip lamp revealed abnormal deposits on the cornea in seven patients, including two asymptomatic patients, who were tested. Based on physical examination, eleven patients aged over 60 years had loose facial skin, facial muscle weakness, and tongue atrophy (Fig. 2). Ophthalmoparesis was observed in three patients. The impairment of joint position sense and vibration sense were found in five patients. However, all patients did not present with muscle weakness of the limbs. Two patients (IV-1 and IV-2) in their 30s had only mild cutis laxa on their face and scalp (Supplementary Fig. 1, only online). Physical examination and needle electromyography also did not show any abnormalities in the tongue and facial muscles of two patients in their 30s. Ten patients underwent nerve conduction studies and needle electromyography. The results showed that three pa-

Table 1. Demographic Data of 13 Korean Patients with AGel Amyloidosis from Three Unrelated Families

Patients						Clinical characteristics							Tests		
Family	Member	Sex	Age at exam (yr)	Age at onset of cutis laxa (yr)	Age at onset of drooping eyelids (yr)	Age at onset of dysarthria (yr)	Decreased visual acuity	Ophthalmoparesis	Facial muscle involve	Tongue atrophy	Limb muscle weakness	Sensory deficits of leg	Drooping eyelids	Slip-lamp	NCS	Brain MRIs
MF1531	III-6	M	76	14	52	65	+	+	+	+	-	+	+	CLA	S	Yes
	III-7	M	74	17	55	65	-	+	+	+	-	+	+	ND	SM	Yes
	III-9	M	76	25	51	70	-	-	+	+	-	-	+	CLA	S	Yes
	III-10	M	73	16	60	70	-	-	+	+	-	-	+	ND	S	Yes
	III-14	M	74	15	54	67	-	+	+	+	-	+	+	CLA	SM	Yes
MF1532	II-6	M	77	30	51	72	-	-	+	+	-	-	+	ND	ND	ND
	III-2	F	64	20	52	62	+	-	+	+	-	-	+	CLA	CTS	Yes
	III-3	M	61	30	47	59	-	-	+	+	-	-	+	ND	CTS	Yes
	IV-1	F	39	15	None	None	-	-	-	-	-	-	-	ND	Normal	ND
	IV-2	M	37	15	None	None	-	-	-	-	-	-	-	ND	Normal	ND
MF1533	III-2	F	78	30	52	72	+	-	+	+	-	+	+	CLA	ND	ND
	III-3	M	75	30	60	66	+	-	+	+	-	+	+	CLA	ND	ND
	III-5	F	67	20	60	60	+	-	+	+	-	-	+	CLA	CTS	Yes

NCS, nerve conduction study; MRI, magnetic resonance imaging; +, present; -, absent; CLA, corneal lattice amyloidosis; ND, not done; S, sensory polyneuropathy; SM, axonal sensorimotor polyneuropathy; CTS, carpal tunnel syndrome.

https://doi.org/10.3349/ymj.2021.62.5.431

Fig. 2. Cutis laxa on the face (A) and tongue atrophy (B-I) in patients with AGel amyloidosis.

tients presented with sensory polyneuropathy, three with carpal tunnel syndrome, and two with axonal sensorimotor polyneuropathy. Meanwhile, two patients had normal study results. In addition, eight patients aged over 60 years showed chronic neurogenic process of the tongue and facial muscles.

Brain MRI findings of Korean patients with AGel amyloidosis

Eight patients aged over 60 years who had AGel amyloidosis and eight age- and sex-matched healthy controls underwent MRI. Axial FLAIR images of the brain showed no significant difference between the patients and healthy controls (Fig. 3). In VBM analysis, the patients had a significant loss of the right middle occipital gyrus, superior frontal gyrus, middle frontal gyrus, and left cerebellum (culmen), compared to healthy controls ($p<0.001$, uncorrected) (Supplementary Fig. 2, only online). However, there was no significant difference between the patients and healthy controls at the corrected significance level. Based on the voxel-wise TBSS analysis, the patients had significantly lower FA values than healthy controls. The results are shown in Supplementary Fig. 3 (only online) ($p<0.05$, uncorrected). However, there was no difference in FDR-corrected results between the two groups. The FreeSurfer analysis did not show any significant difference in cortical thickness between the patients and healthy controls at both uncorrected and corrected significance levels.

DISCUSSION

Our study outlines the clinical characteristics and brain structural abnormalities among Korean patients with AGel amyloidosis, in which the cranial and peripheral nerves were mainly affected. In addition, this study assessed the brain parenchymal abnormalities among patients with AGel amyloidosis using the VBM, TBSS, and FreeSurfer (cortical thickness measure-

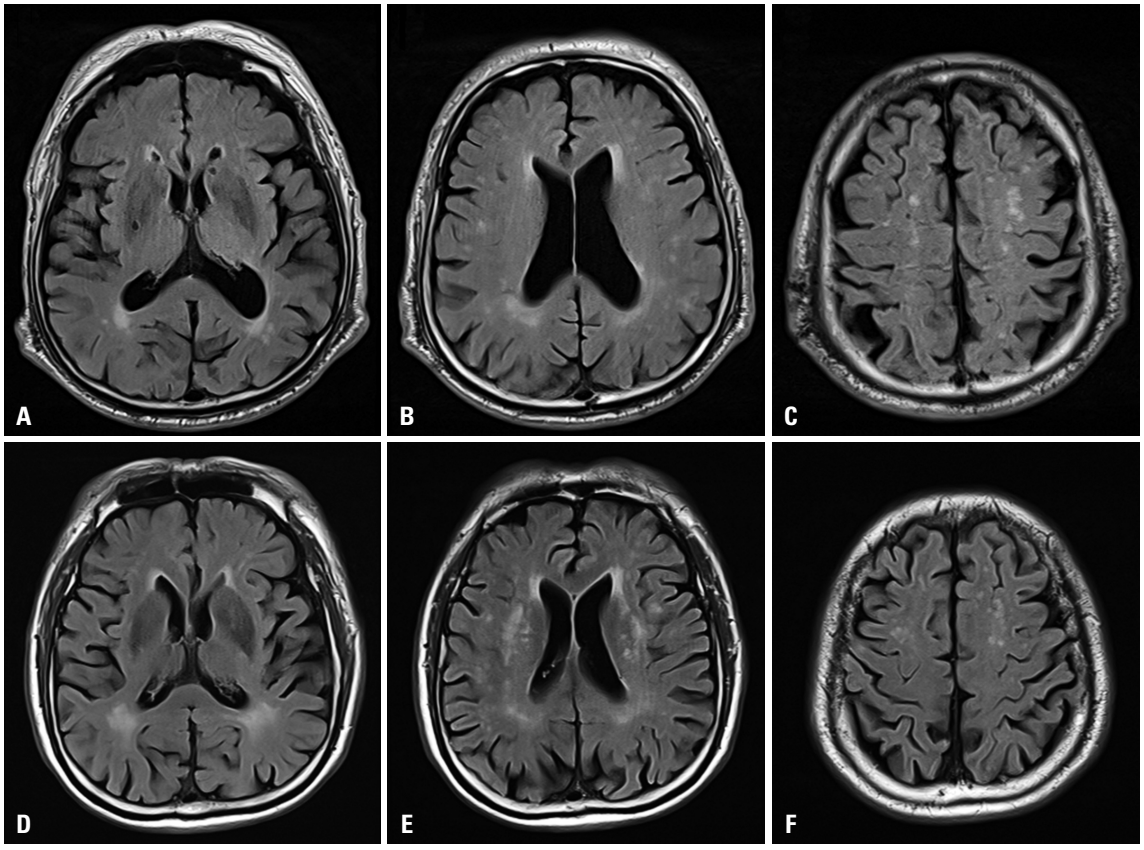

Fig. 3. Axial fluid-attenuated inversion recovery MR images of III-6 patient from MF1531 and age- and sex-matched healthy controls. There were no significant differences in white matter changes between patients with AGel amyloidosis (A-C) and healthy controls (D-F).

ments) techniques.

Our patients had the same pathogenic variant in the *GSN* gene (NM_000177.5: c.640G>T; NP_000168.1: p.D214Y). In previous literature, this amino acid change was historically referred to as p.D187Y (www.omim.org/entry/137350#0002).[5] This pathogenic variant is the same variant previously reported in Korean patients with AGel amyloidosis.[16,17] Two main pathogenic variants (c.640G>A and c.640G>T) affect the same codon. The central hypothesis is as follows: these pathogenic variants result in aberrant conformational changes and disrupt the Ca^{2+} binding capacity of the gelsolin protein. This alteration leads to aberrant furin cleavage in the trans-Golgi network and triggers the proteolytic pathway producing amyloidogenic fragments.[30,31] A recent study also showed that the D214N AGel protein under Ca^{2+}-depletion and a low pH condition can induce amyloid-like assembly without the specific proteolytic step.[32] However, although alterations in the *GSN* gene do not always result in systemic amyloidosis, some have been shown to cause renal amyloidosis. Two pathogenic variants (c.580G>A and c.633C>A) were observed in renal amyloidosis without dermatologic, neurological, and ophthalmologic abnormalities.[33,34] Therefore, further studies must be conducted to determine the pathological mechanism by which the variants in the *GSN* gene cause the clinical phenotype.

Our patients showed prominent bulbar palsy and early-onset cutis laxa. Prominent bulbar palsy is not a common feature in patients with the c.640G>A variant.[3] For example, dysarthria, a typical symptom of bulbar palsy, was observed in only 61 (27%) of 227 Finish patients with the c.640G>A variant.[3] However, 11 (65%) of 17 patients with the c.640G>T variant had dysarthria, dysphagia, or tongue atrophy.[14,15,18,35,36] Therefore, prominent bulbar palsy could be considered a characteristic finding of patients with the c.640G>T variant, like our patients. Early-onset cutis laxa was not previously reported in studies from other countries.[4-15,18,35,36] The age at onset of cutis laxa was based on the patient's memory. However, the patients first noticed their loose scalp when they cut their hair using hair clippers as teenagers. Moreover, we found cutis laxa of the face in two patients in their 30s. Further studies are needed regarding this finding. Only 38% of the patients complained of decreased visual acuity. However, analysis using a slip lamp revealed corneal dystrophy in all tested patients. Ophthalmoparesis was not found in Korean patients, but was previously observed in patients with AGel amyloidosis.[37]

Our study showed no significant differences in cerebral abnormalities between the patients and healthy controls (FDR-corrected $p<0.05$). To date, few studies have assessed brain damage in patients with AGel amyloidosis.[19,20,38] Among them,

https://doi.org/10.3349/ymj.2021.62.5.431

one study revealed frontal leukoencephalopathy, as well as periventricular and intrapontine high signal intensities, on brain MRI.[38] Other studies also showed cerebral amyloid angiopathy in autopsy cases.[19,20] To confirm these differences, we analyzed multimodal structural brain images: VBM, TBSS, and FreeSurfer. However, none of the anatomical brain analyses revealed a significant loss of GM and WM in patients. For uncorrected results, the analysis of VBM and TBSS showed the loss of several cerebral regions in patients. However, there were no significant differences between the patients and healthy controls at the corrected significance level. Additionally, the reduced regions in patients at uncorrected results were not associated with the neurological deficits of AGel amyloidosis. Therefore, we did not find additional cerebral abnormalities associated with cranial neuropathy of AGel amyloidosis. Together with previous studies, our results suggest that there were less cerebral abnormalities rather than no involvement.

Our study had a significant limitation of including only a small number of patients with AGel amyloidosis. We analyzed the clinical information of 13 patients with AGel amyloidosis and brain MRI findings of eight patients. Since AGel amyloidosis is a rare genetic disease, it was only observed in two Korean patients previously.[16,17] To overcome this limitation, we included age- and sex-matched healthy controls. However, further stud¬ies with a larger cohort must be conducted to validate the consistency of our results.

In conclusion, this study outlined the characteristic clinical manifestations of prominent bulbar palsy and early-onset cutis laxa in 13 Korean patients with AGel amyloidosis. Additionally, we confirmed that AGel amyloidosis mainly affected the peripheral nervous system rather than the central nervous system.

ACKNOWLEDGEMENTS

This study was supported by a new faculty research seed money grant of Yonsei University College of Medicine for 2020 (3-2020-0127).

AUTHOR CONTRIBUTIONS

Conceptualization: Young-Chul Choi, Woo Hyun Shim, and Hyung Jun Park. Data curation: E-Nae Cheong, Wooyul Paik, Young-Min Lim, and Hyunjin Kim. Formal analysis: E-Nae Cheong and Wooyul Paik. Funding acquisition: Hyung Jun Park. Supervision: Young-Chul Choi. Writing—original draft: E-Nae Cheong and Hyung Jun Park. Approval of final manuscript: all authors.

ORCID iDs

E-Nae Cheong https://orcid.org/0000-0003-1270-5385
Wooyul Paik https://orcid.org/0000-0001-9617-6227
Young-Chul Choi https://orcid.org/0000-0001-5525-6861
Young-Min Lim https://orcid.org/0000-0001-5074-812X
Hyunjin Kim https://orcid.org/0000-0003-0264-4531
Woo Hyun Shim https://orcid.org/0000-0002-7251-2916
Hyung Jun Park https://orcid.org/0000-0003-4165-8901

REFERENCES

1. Maury CP. Gelsolin-related amyloidosis. Identification of the amyloid protein in Finnish hereditary amyloidosis as a fragment of variant gelsolin. J Clin Invest 1991;87:1195-9.
2. Meretoja J. Familial systemic paramyloidosis with lattice dystrophy of the cornea, progressive cranial neuropathy, skin changes and various internal symptoms. A previously unrecognized heritable syndrome. Ann Clin Res 1969;1:314-24.
3. Nikoskinen T, Schmidt EK, Strbian D, Kiuru-Enari S, Atula S. Natural course of Finnish gelsolin amyloidosis. Ann Med 2015;47:506-11.
4. Mustonen T, Schmidt EK, Valori M, Tienari PJ, Atula S, Kiuru-Enari S. Common origin of the gelsolin gene variant in 62 Finnish AGel amyloidosis families. Eur J Hum Genet 2018;26:117-23.
5. de la Chapelle A, Tolvanen R, Boysen G, Santavy J, Bleeker-Wagemakers L, Maury CP, et al. Gelsolin-derived familial amyloidosis caused by asparagine or tyrosine substitution for aspartic acid at residue 187. Nat Genet 1992;2:157-60.
6. Rothstein A, Auran JD, Wittpenn JR, Koester CJ, Florakis GJ. Confocal microscopy in Meretoja syndrome. Cornea 2002;21:364-7.
7. Taira M, Ishiura H, Mitsui J, Takahashi Y, Hayashi T, Shimizu J, et al. Clinical features and haplotype analysis of newly identified Japanese patients with gelsolin-related familial amyloidosis of Finnish type. Neurogenetics 2012;13:237-43.
8. Stewart HS, Parveen R, Ridgway AE, Bonshek R, Black GC. Late onset lattice corneal dystrophy with systemic familial amyloidosis, amyloidosis V, in an English family. Br J Ophthalmol 2000;84:390-4.
9. Conceição I, Sales-Luis ML, De Carvalho M, Evangelista T, Fernandes R, Paunio T, et al. Gelsolin-related familial amyloidosis, Finnish type, in a Portuguese family: clinical and neurophysiological studies. Muscle Nerve 2003;28:715-21.
10. Ardalan MR, Shoja MM, Kiuru-Enari S. Amyloidosis-related nephrotic syndrome due to a G654A gelsolin mutation: the first report from the Middle East. Nephrol Dial Transplant 2007;22:272-5.
11. Huerva V, Velasco A, Sánchez MC, Mateo AJ, Matías-Guiu X. Lattice corneal dystrophy type II: clinical, pathologic, and molecular study in a Spanish family. Eur J Ophthalmol 2007;17:424-9.
12. Carrwik C, Stenevi U. Lattice corneal dystrophy, gelsolin type (Meretoja's syndrome). Acta ophthalmol 2009;87:813-9.
13. Lüttmann RJ, Teismann I, Husstedt IW, Ringelstein EB, Kuhlenbäumer G. Hereditary amyloidosis of the Finnish type in a German family: clinical and electrophysiological presentation. Muscle Nerve 2010;41:679-84.
14. Chastan N, Baert-Desurmont S, Saugier-Veber P, Dérumeaux G, Cabot A, Frébourg T, et al. Cardiac conduction alterations in a French family with amyloidosis of the Finnish type with the p.Asp-187Tyr mutation in the GSN gene. Muscle Nerve 2006;33:113-9.
15. Solari HP, Ventura MP, Antecka E, Belfort Junior R, Burnier MN Jr. Danish type gelsolin-related amyloidosis in a Brazilian family: case reports. Arq Bras Oftalmol 2011;74:286-8.
16. Park KJ, Park JH, Park JH, Cho EB, Kim BJ, Kim JW. The first Korean family with hereditary gelsolin amyloidosis caused by p.D214Y mutation in the GSN gene. Ann Lab Med 2016;36:259-62.
17. Kim TH, Bae JH, Lim DH, Chung ES, Chung TY. Lattice corneal dystrophy, gelsolin type: the first case report in Korea. J Korean Ophthalmol Soc 2013;54:667-70.
18. Caress JB, Johnson JO, Abramzon YA, Hawkins GA, Gibbs JR, Sullivan EA, et al. Exome sequencing establishes a gelsolin mutation

as the cause of inherited bulbar-onset neuropathy. Muscle Nerve 2017;56:1001-5.
19. Kiuru S, Salonen O, Haltia M. Gelsolin-related spinal and cerebral amyloid angiopathy. Ann Neurol 1999;45:305-11.
20. Makishita H, Ikeda S-I, Yazaki M, Yamane M, Yumoto K-K, Maury C, et al. Postmortem pathological findings in a Japanese patient with familial amyloidosis, Finnish type (FAF). Amyloid 1996;3:134-9.
21. Bodini B, Khaleeli Z, Cercignani M, Miller DH, Thompson AJ, Ciccarelli O. Exploring the relationship between white matter and gray matter damage in early primary progressive multiple sclerosis: an in vivo study with TBSS and VBM. Hum Brain Mapp 2009;30:2852-61.
22. Virtanen SM, Lindroos MM, Majamaa K, Nuutila P, Borra RJ, Parkkola R. Voxelwise analysis of diffusion tensor imaging and structural MR imaging in patients with the m.3243A>G mutation in mitochondrial DNA. AJNR Am J Neuroradiol 2011;32:522-6.
23. Nir TM, Jahanshad N, Villalon-Reina JE, Toga AW, Jack CR, Weiner MW, et al. Effectiveness of regional DTI measures in distinguishing Alzheimer's disease, MCI, and normal aging. NeuroImage Clin 2013;3:180-95.
24. Menke RA, Scholz J, Miller KL, Deoni S, Jbabdi S, Matthews PM, et al. MRI characteristics of the substantia nigra in Parkinson's disease: a combined quantitative T1 and DTI study. Neuroimage 2009;47:435-41.
25. Zanigni S, Evangelisti S, Giannoccaro MP, Oppi F, Poda R, Giorgio A, et al. Relationship of white and gray matter abnormalities to clinical and genetic features in myotonic dystrophy type 1. NeuroImage Clin 2016;11:678-85.
26. Paavilainen T, Lepomäki V, Saunavaara J, Borra R, Nuutila P, Kantola I, et al. Diffusion tensor imaging and brain volumetry in Fabry disease patients. Neuroradiology 2013;55:551-8.
27. Park JS, Song H, Jang KE, Cha H, Lee SH, Hwang SK, et al. Diffusion tensor imaging and voxel-based morphometry reveal corticospinal tract involvement in the motor dysfunction of adult-onset myotonic dystrophy type 1. Sci Rep 2018;8:15592.
28. Levy E, Haltia M, Fernandez-Madrid I, Koivunen O, Ghiso J, Prelli F, et al. Mutation in gelsolin gene in Finnish hereditary amyloidosis. J Exp Med 1990;172:1865-7.
29. Ashburner J. A fast diffeomorphic image registration algorithm. Neuroimage 2007;38:95-113.
30. Solomon JP, Page LJ, Balch WE, Kelly JW. Gelsolin amyloidosis: genetics, biochemistry, pathology and possible strategies for therapeutic intervention. Crit Rev Biochem Mol Biol 2012;47:282-96.
31. Chen CD, Huff ME, Matteson J, Page L, Phillips R, Kelly JW, et al. Furin initiates gelsolin familial amyloidosis in the Golgi through a defect in Ca2+ stabilization. EMBO J 2001;20:6277-87.
32. Srivastava A, Singh J, Singh Yadav SP, Arya P, Kalim F, Rose P, et al. The gelsolin pathogenic D187N mutant exhibits altered conformational stability and forms amyloidogenic oligomers. Biochemistry 2018;57:2359-72.
33. Sethi S, Theis JD, Quint P, Maierhofer W, Kurtin PJ, Dogan A, et al. Renal amyloidosis associated with a novel sequence variant of gelsolin. Am J Kidney Dis 2013;61:161-6.
34. Efebera YA, Sturm A, Baack EC, Hofmeister CC, Satoskar A, Nadasdy T, et al. Novel gelsolin variant as the cause of nephrotic syndrome and renal amyloidosis in a large kindred. Amyloid 2014;21:110-2.
35. Boysen G, Galassi G, Kamieniecka Z, Schlaeger J, Trojaborg W. Familial amyloidosis with cranial neuropathy and corneal lattice dystrophy. J Neurol Neurosurg Psychiatry 1979;42:1020-30.
36. Contégal F, Bidot S, Thauvin C, Lévèque L, Soichot P, Gras P, et al. Finnish amyloid polyneuropathy in a French patient. Rev Neurol (Paris) 2006;162:997-1001.
37. Pihlamaa T, Salmi T, Suominen S, Kiuru-Enari S. Progressive cranial nerve involvement and grading of facial paralysis in gelsolin amyloidosis. Muscle Nerve 2016;53:762-9.
38. Kiuru S, Seppäläinen AM, Salonen O, Hokkanen L, Somer H, Palo J. CNS abnormalities in patients with familial amyloidosis, Finnish type (FAF). Amyloid 1995;2:22-30.

https://doi.org/10.3349/ymj.2021.62.5.431